复合材料学报 第32卷 第3期 6月 2015年
Acta Materiae Compositae Sinica Vol. 32 No. 3 June 2015

**DOI**：10.13801/j.cnki.fhclxb.20150303.001

# 有限高磁电弹性体中双半动态与静态裂纹分析

郭怀民*，赵国忠
（包头师范学院 数学科学学院，包头 014030）

**摘 要**：狭长体中的裂纹是断裂力学中经常采用的研究模型。含有共线无限长裂纹的条形磁电弹性体，当面内的力电磁和反平面的剪应力作用在左边裂纹尖端附近的一段裂纹面上时，往往会产生动态断裂。利用复变函数法中的拱形变换公式，导出了磁电全非渗透型边界条件下左裂纹尖端动态的应力强度因子以及机械应变能释放率的解析解。当运动速度趋于零时退化为静止状态下的解。通过数值算例分析了断裂机理，讨论了静止状态下狭长体和裂纹的几何尺寸、外力、电场和磁场分别对能量释放率的影响，为相关器件的设计与制造提供了帮助。

**关键词**：运动裂纹；磁电弹性复合材料；复变函数法；应力强度因子；机械应变能释放率
**中图分类号**：TB330.1；O346.1 **文献标志码**：A **文章编号**：1000-3851(2015)03-0888-08

由于磁致伸缩材料和压电材料混合而成的磁电复合材料可以将能量在力、磁、电之间相互转化[1]，近年来成为人们研究的热点。对于 $BaTiO_3$-$CoFe_2O_4$ 磁电复合材料，其力-电耦合与磁-力耦合相互作用可以实现磁信号和电场信号之间的相互转化，耦合系数比磁电单相材料高出许多，因此压电压磁复合材料更广泛地应用于制造人工智能电子器件、制动器，水听器和数码相机等。已有许多学者致力于研究压电压磁复合材料的磁-电-弹性场的相互耦合作用及其物理力学特性。磁电材料的磁电效应往往受材料的性质、构型及边界条件等因素的影响，在材料的制备过程中，各种微观或宏观缺陷不可避免会存在。研究各种缺陷对材料宏观性能的影响，有助于设计、制造更标准的器件。文献[2-14]对磁电弹性复合材料基体中存在的各种缺陷进行研究，并取得了较多研究成果。比如 Hou 和 Leung[2] 研究了内含椭圆夹杂的无限磁电介质受到面内和面外剪切作用的情形，给出了圆形裂纹前沿的磁、电、弹性场的分步。Wang 和 Shen[3] 对磁电材料中含有的若干夹杂问题进行了研究，并得到了解析解。Liu 等[4] 研究了含裂纹及孔洞的磁电弹性复合材料的 Green 函数。Soh 和 Liu[7] 研究了 2 个磁电弹性体的边界裂纹问题，给出了磁电弹性场的解析解。文献[8]讨论了条形磁电弹性体中 III 型单边无限长裂纹的场强度因子，分析了受载裂纹长度、狭长体高度以及电、磁和机械能对能量释放率的影响。Hu 和 Zhong[9] 利用 Fourier 变换方法分析了裂纹运动速度对裂纹扩展的影响。Singh 等[11] 利用积分变换法给出了磁电弹性复合材料中双裂纹的解析解。胡克强等[12] 基于线性电磁弹性理论，进行了压电-压磁板条中反平面裂纹的电-磁-弹性分析，获得了裂纹尖端附近应力、应变、电位移、电场和磁场的封闭表达式。卢子兴等[13] 讨论了含双半无限裂纹的压电狭长体中部分裂纹面上受力及电载荷的问题。刘萍等[14] 研究了含单边无限裂纹的压电狭长体中部分裂纹面上受力、电载荷作用下的运动裂纹问题。

目前文献中对于更加复杂的磁电弹性复合材料狭长体中含共线双半无限运动裂纹问题的研究鲜有报道。本文采用磁电全非渗透型边界条件假设，结合拱形变换公式等方法，导出了力、电场、磁场共同作用在部分裂纹面上时，裂纹尖端的场强度因子和机械应变能释放率的解析解。通过举例计算和图像分析，给出了静止状态下磁电弹性狭长体和裂纹的几何尺寸、力、电场和磁场对能量释放率的影响规律。

**收稿日期**：2014-12-22；**录用日期**：2015-01-30；**网络出版时间**：2015-03-03 08:13
**网络出版地址**：www.cnki.net/kcms/detail/11.1801.TB.20150303.0813.001.html
**基金项目**：国家自然科学基金（11261035）；内蒙古自然科学基金(2012MS0102)
**通讯作者**：郭怀民，硕士，副教授，研究方向为复合材料力学。 E-mail：ghmin@163.com

***引用格式***：*郭怀民，赵国忠. 有限高磁电弹性体中双半动态与静态裂纹分析[J]. 复合材料学报，2015，32(3)：888-895. Guo H M，Zhao G Z. Dynamic and static analysis for two semi-infinite cracks in finite magnetoelectroelastic strip[J]. Acta Materiae Compositae Sinica，2015，32(3)：888-895.*

## 1 问题描述

图 1 为狭长磁电弹性复合材料体中双半无限裂纹。$x_3$ 轴对应的是磁电弹性介质的磁电极化方向，沿 $x_1$-$x_2$ 平面各向是同性的，该基体中有一对共线的无限长裂纹，裂纹面到材料体上、下表面的高度都是 $H$。$L$ 为两条裂纹之间的距离。当左边裂纹尖端附近长度为 $a$ 的一段上作用有面内电载荷 $D_0$、磁载荷 $B_0$ 及反平面剪应力 $\tau_0$ 且裂纹面上的载荷与裂纹尖端都以匀速 $v$ 沿 $x_1$ 轴方向运动时，与裂纹一起运动的坐标系为 $(x_1, x_2, x_3)$，同时建立一个固定坐标系 $(x, y, z)$。边界条件可表示为

$$\begin{cases} x_2 = \pm H \quad -\infty < x_1 < +\infty: \\ \quad [\sigma_{32}\ D_2\ B_2]^{\mathrm{T}} = \mathbf{0} \\ x_2 = 0 \quad -\infty < x_1 < -a, L < x_1 < +\infty: \\ \quad [\sigma_{32}\ D_2\ B_2]^{\mathrm{T}} = \mathbf{0} \\ x_2 = 0 \quad -a < x_1 < 0: [\sigma_{32}\ D_2\ B_2]^{\mathrm{T}} = \\ \quad [-\tau_0\ D_0\ B_0]^{\mathrm{T}} \\ x_1 = \pm\infty \quad -H < x_2 < +H: [\sigma_{32}\ D_2\ B_2]^{\mathrm{T}} = \mathbf{0} \end{cases} \tag{1}$$

这时，所有变量和 $z$ 就没有关系了，其本构方程为

$$\begin{bmatrix} \sigma_{3k} \\ D_k \\ B_k \end{bmatrix} = \begin{bmatrix} c_{44} & e_{15} & q_{15} \\ e_{15} & -\kappa_{11} & -d_{11} \\ q_{15} & -d_{11} & -\mu_{11} \end{bmatrix} \begin{bmatrix} w_{3,k} \\ \varphi_{,k} \\ \psi_{,k} \end{bmatrix} \quad k = 1,2 \tag{2}$$

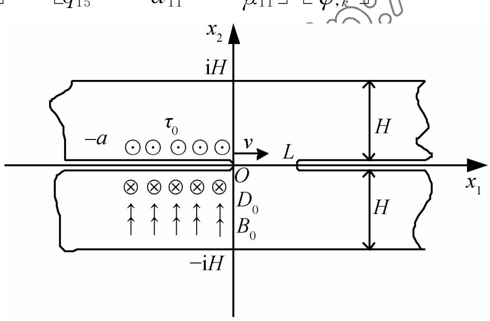


图 1 狭长磁电弹性复合材料体中双半无限裂纹

Fig. 1 Two semi-infinite cracks in magnetoelectroelastic composite strip

若不考虑体力、体电荷密度和体电流的作用，动态位移分量、电势和磁势满足的微分方程组为

$$\begin{cases} c_{44}\nabla^2 w + e_{15}\nabla^2\varphi + q_{15}\nabla^2\psi = \rho\dfrac{\partial^2 w}{\partial t^2} \\ e_{15}\nabla^2 w - \kappa_{11}\nabla^2\varphi - d_{11}\nabla^2\psi = 0 \\ q_{15}\nabla^2 w - d_{11}\nabla^2\varphi - \mu_{11}\nabla^2\psi = 0 \end{cases} \tag{3}$$

式中：$\nabla^2 = \dfrac{\partial^2}{\partial x_1^2} + \dfrac{\partial^2}{\partial x_2^2}$；$w$、$D$、$\sigma_{ij}$、$\varphi$ 和 $\psi$ 依次为反平面位移、电位移、应力、面内电势和面内磁势；$\rho$ 为磁电弹性介质的质量密度；$\kappa_{11}$、$c_{44}$、$e_{15}$、$q_{15}$ 依次为介电常数、材料常数、压电常数、磁电常数；$\mu_{11}$ 和 $d_{11}$ 分别表示磁导率和磁电耦合常数。

引入新函数

$$\begin{cases} \varphi = \zeta - \dfrac{d_{11}}{\kappa_{11}}\eta + \dfrac{e_{15}\mu_{11} - q_{15}d_{11}}{\kappa_{11}\mu_{11} - d_{11}^2}w \\ \psi = \eta - \dfrac{d_{11}}{\eta_{11}}\zeta + \dfrac{q_{15}\kappa_{11} - e_{15}d_{11}}{\kappa_{11}\mu_{11} - d_{11}^2}w \end{cases} \tag{4}$$

式中：$\zeta$ 和 $\eta$ 为两个辅助函数。假设裂纹以匀速扩展，则起始坐标和运动坐标的关系为

$$\begin{cases} x = x_1 - vt \\ y = x_2 \\ z = x_3 \end{cases} \tag{5}$$

由式(5)，方程组(3)可化为 3 个耦合的方程：

$$\begin{cases} \dfrac{\partial^2 w}{\partial x^2} + \dfrac{\partial^2 w}{\partial y_1^2} = 0 \\ \nabla^2\zeta = 0 \\ \nabla^2\eta = 0 \end{cases} \tag{6}$$

其中：

$$\begin{cases} y_1 = \alpha_1 y,\ \alpha_1 = \sqrt{1 - \dfrac{v^2}{c^2}},\ c = \sqrt{c_e/\rho} \\ c_e = c_{44} + \dfrac{\kappa_{11}(q_{15})^2 + \mu_{11}(e_{15})^2 - 2q_{15}e_{15}d_{11}}{\kappa_{11}\mu_{11} - (d_{11})^2} \end{cases}$$

式中：$c$ 为对应的磁电弹性介质的反平面剪切波的波速；$c_e$ 是与材料常数有关的量。由式(6)，式(4)可进一步化为

$$\begin{cases} \dfrac{\partial^2 w}{\partial x^2} + \dfrac{\partial^2 w}{\partial y_1^2} = 0 \\ \dfrac{\partial^2 \varphi}{\partial x^2} + \dfrac{\partial^2 \varphi}{\partial y_1^2} = 0 \\ \dfrac{\partial^2 \psi}{\partial x^2} + \dfrac{\partial^2 \psi}{\partial y_1^2} = 0 \end{cases} \tag{7}$$

以式(6)的解作为某解析函数的实部或虚部，该解析函数形式记为 $U_1(z_1)$、$\Phi_1(z)$、$\Psi_1(z)$。

其中：

$$z_1 = x + \mathrm{i}y_1,\ z = x + \mathrm{i}y$$

这样有：

$$\begin{cases} w(x,y) = \mathrm{Re}\,U_1(z_1) \\ \varphi(x,y) = \mathrm{Re}\,\Phi_1(z) \\ \psi(x,y) = \mathrm{Re}\,\Psi_1(z) \end{cases} \tag{8}$$

将式(8)代入本构方程式(2)得

$$
\begin{cases}
\sigma_{13} = \dfrac{1}{2}[c_{44}(U'_1 + \overline{U'_1}) + e_{15}(\Phi'_1 + \overline{\Phi'_1}) + \\
\qquad q_{15}(\Psi'_1 + \overline{\Psi'_1})] \\
\sigma_{23} = \dfrac{\mathrm{i}}{2}[\alpha_1 c_{44}(U'_1 - \overline{U'_1}) + e_{15}(\Phi'_1 - \overline{\Phi'_1}) + \\
\qquad q_{15}(\Psi'_1 - \overline{\Psi'_1})] \\
D_1 = \dfrac{1}{2}[e_{15}(U'_1 + \overline{U'_1}) - \kappa_{11}(\Phi'_1 + \overline{\Phi'_1}) - \\
\qquad d_{11}(\Psi'_1 + \overline{\Psi'_1})] \\
D_2 = \dfrac{\mathrm{i}}{2}[\alpha_1 e_{15}(U'_1 - \overline{U'_1}) - \kappa_{11}(\Phi'_1 - \overline{\Phi'_1}) - \\
\qquad d_{11}(\Psi'_1 - \overline{\Psi'_1})] \\
B_1 = \dfrac{1}{2}[q_{15}(U'_1 + \overline{U'_1}) - d_{11}(\Phi'_1 + \overline{\Phi'_1}) - \\
\qquad \mu_{11}(\Psi'_1 + \overline{\Psi'_1})] \\
B_2 = \dfrac{\mathrm{i}}{2}[\alpha_1 q_{15}(U'_1 - \overline{U'_1}) - d_{11}(\Phi'_1 - \overline{\Phi'_1}) - \\
\qquad \mu_{11}(\Psi'_1 - \overline{\Psi'_1})]
\end{cases}
\tag{9}
$$

再由边界条件(1)可得

$$
\begin{cases}
\alpha_1 c_{44}(U'_1 - \overline{U'_1}) + e_{15}(\Phi'_1 - \overline{\Phi'_1}) + \\
\qquad q_{15}(\Psi'_1 - \overline{\Psi'_1}) = 2\mathrm{i}\tau_0 \\
\alpha_1 e_{15}(U'_1 - \overline{U'_1}) - \kappa_{11}(\Phi'_1 - \overline{\Phi'_1}) - \\
\qquad d_{11}(\Psi'_1 - \overline{\Psi'_1}) = -2\mathrm{i}D_0 \\
\alpha_1 e_{15}(U'_1 - \overline{U'_1}) - d_{11}(\Phi'_1 - \overline{\Phi'_1}) - \\
\qquad \mu_{11}(\Psi'_1 - \overline{\Psi'_1}) = -2\mathrm{i}B_0
\end{cases}
\tag{10}
$$

## 2　问题求解

### 2.1　引入拱形变换公式

拱形变换公式为[15]

$$
z_1, z = \omega(\zeta) = \frac{H}{\pi}\ln\frac{1+\alpha\left(\dfrac{1-\zeta}{1+\zeta}\right)^2}{1+\gamma\alpha\left(\dfrac{1-\zeta}{1+\zeta}\right)^2}
\tag{11}
$$

其中：

$$
\begin{cases}
\alpha = \dfrac{1-\mathrm{e}^{\frac{-\pi a}{H}}}{1-\mathrm{e}^{\frac{-\pi(a+L)}{H}}} \\
\gamma = \mathrm{e}^{\frac{-\pi L}{H}}
\end{cases}
$$

该变换把 $z$ 平面上的区域映射到 $\zeta$ 平面上单位圆的内部。且 $\omega(1)=0$，$\omega(-1)=-L$，$\omega(\mathrm{i})=-a-0\mathrm{i}$，$\omega(-\mathrm{i})=-a+0\mathrm{i}$。$\alpha$ 与 $\gamma$ 不仅具有几何意义，也有物理意义，代表裂纹间相互作用的因子。其逆变换为

$$
\zeta = \omega^{-1}(z) = \frac{\sqrt{\alpha}-\sqrt{\dfrac{\mathrm{e}^{\frac{\pi z}{H}}-1}{1-\gamma\mathrm{e}^{\frac{\pi z}{H}}}}}{1-\gamma\mathrm{e}^{\frac{\pi z}{H}}}
\tag{12}
$$

引入记号

$$
\begin{cases}
U_1(z_1) = U_1[\omega(\zeta)] = U(\zeta) \\
\Phi_1(z_1) = \Phi_1[\omega(\zeta)] = \Phi(\zeta) \\
\Psi_1(z_1) = \Psi_1[\omega(\zeta)] = \Psi(\zeta) \\
U'_1(z_1) = \dfrac{U'(\zeta)}{\omega'(\zeta)} \\
\Phi'_1(z_1) = \dfrac{\Phi'(\zeta)}{\omega'(\zeta)} \\
\Psi'_1(z_1) = \dfrac{\Psi'(\zeta)}{\omega'(\zeta)}
\end{cases}
\tag{13}
$$

将式(12)代入式(9)并在两边分别乘以 $\dfrac{\omega'(\sigma)}{(\sigma-\zeta)}$，两边再做 Cauchy 积分($\sigma$ 为在 $|\zeta|<1$ 中的任意一点)，得

$$
\begin{cases}
\alpha_1 U'(\zeta) + \dfrac{e_{15}}{c_{44}}\Phi'(\zeta) + \dfrac{q_{15}}{c_{44}}\Psi'(\zeta) = F(\zeta)\cdot\dfrac{2\mathrm{i}\tau_0}{c_{44}} \\
\Phi'(\zeta) - \dfrac{e_{15}}{\kappa_{11}}\alpha_1 U'(\zeta) + \dfrac{d_{11}}{\kappa_{11}}\Psi'(\zeta) = F(\zeta)\cdot\dfrac{2\mathrm{i}D_0}{\kappa_{11}} \\
\Psi'(\zeta) - \dfrac{e_{15}}{\mu_{11}}\alpha_1 U'(\zeta) + \dfrac{d_{11}}{\mu_{11}}\Phi'(\zeta) = F(\zeta)\cdot\dfrac{2\mathrm{i}B_0}{\mu_{11}} \\
\boldsymbol{K}_{\mathrm{III}} = \alpha\begin{bmatrix}\tau_0 \\ D_0 \\ B_0\end{bmatrix}\dfrac{\sqrt{2H}}{\pi\sqrt{1-\gamma}}\Big[\ln\dfrac{1+\sqrt{\alpha}}{1-\sqrt{\alpha}} - \\
\qquad \sqrt{\gamma}\ln\dfrac{1+\sqrt{\alpha\gamma}}{1-\sqrt{\alpha\gamma}}\Big]
\end{cases}
\tag{14}
$$

求解式(14)并代入式(8)得到

$$
\begin{cases}
\sigma_{13} - \mathrm{i}\sigma_{23} = \dfrac{c_{44}}{2}[(1+\alpha_1)U'_1 + (1-\alpha_1)\overline{U'_1}] + \\
\qquad e_{15}\Phi'_1 + q_{15}\Psi'_1 = \mathrm{i}\Big[\dfrac{C_1F(\zeta)}{\omega'(\zeta)} + C_2\dfrac{\overline{F(\zeta)}}{\overline{\omega'(\zeta)}}\Big] \\
D_1 - \mathrm{i}D_2 = \dfrac{e_{15}}{2}[(1+\alpha_1)U'_1 + (1-\alpha_1)\overline{U'_1}] - \\
\qquad \kappa_{11}\Phi'_1 - d_{11}\Psi'_1 = \mathrm{i}\Big[\dfrac{C_3F(\zeta)}{\omega'(\zeta)} + C_4\dfrac{\overline{F(\zeta)}}{\overline{\omega'(\zeta)}}\Big] \\
B_1 - \mathrm{i}B_2 = \dfrac{q_{15}}{2}[(1+\alpha_1)U'_1 + (1-\alpha_1)\overline{U'_1}] - \\
\qquad d_{11}\Phi'_1 - \mu_{11}\Psi'_1 = \mathrm{i}\Big[\dfrac{C_5F(\zeta)}{\omega'(\zeta)} + C_6\dfrac{\overline{F(\zeta)}}{\overline{\omega'(\zeta)}}\Big]
\end{cases}
\tag{15}
$$

其中：

$$
\begin{aligned}
C_1 = {} & \{c_{44}\left(1+\frac{1}{\alpha_1}\right)[\tau_0(\kappa_{11}\mu_{11}-d_{11}^2)-e_{15}(D_0\mu_{11}- \\
& B_0 d_{11})+q_{15}(D_0 d_{11}-B_0\kappa_{11})]+2e_{15}[c_{44}(D_0\mu_{11}- \\
& B_0 d_{11})+\tau_0 e_{15}(\mu_{11}-d_{11})+q_{15}e_{15}(D_0-B_0)]+ \\
& 2q_{15}[c_{44}(\kappa_{11}B_0-d_{11}D_0)+e_{15}^2(B_0-D_0)+ \\
& \tau_0 e_{15}(\kappa_{11}-d_{11})]\}\ /\ [c_{44}(\kappa_{11}\mu_{11}-d_{11}^2)+ \\
& e_{15}^2(\mu_{11}-d_{11})+q_{15}e_{15}(\kappa_{11}-d_{11})]
\end{aligned}
$$

$$
\begin{aligned}
C_2 = {} & c_{44}\left(1-\frac{1}{\alpha_1}\right)[\tau_0(\kappa_{11}\mu_{11}-d_{11}^2)-e_{15}(D_0\mu_{11}- \\
& B_0 d_{11})+q_{15}(D_0 d_{11}-B_0 k_{11})]/[c_{44}(k_{11}\mu_{11}- \\
& d_{11}^2)+e_{15}^2(\mu_{11}-d_{11})+q_{15}e_{15}(k_{11}-d_{11})]
\end{aligned}
$$

$$
\begin{aligned}
C_3 = {} & \{e_{15}\left(1+\frac{1}{\alpha_1}\right)[\tau_0(\kappa_{11}\mu_{11}-d_{11}^2)-e_{15}(D_0\mu_{11}- \\
& B_0 d_{11})+q_{15}(D_0 d_{11}-B_0\kappa_{11})]-2\kappa_{11}[c_{44}(D_0\mu_{11}- \\
& B_0 d_{11})+\tau_0 e_{15}(\mu_{11}-d_{11})+q_{15}e_{15}(D_0- \\
& B_0)]-2d_{11}[c_{44}(\kappa_{11}B_0-d_{11}D_0)+e_{15}^2(B_0- \\
& D_0)+\tau_0 e_{15}(\kappa_{11}-d_{11})]\}/[c_{44}(\kappa_{11}\mu_{11}-d_{11}^2)+ \\
& e_{15}^2(\mu_{11}-d_{11})+q_{15}e_{15}(\kappa_{11}-d_{11})]
\end{aligned}
$$

$$
\begin{aligned}
C_4 = {} & e_{15}\left(1-\frac{1}{\alpha_1}\right)[\tau_0(\kappa_{11}\mu_{11}-d_{11}^2)-e_{15}(D_0\mu_{11}- \\
& B_0 d_{11})+q_{15}(D_0 d_{11}-B_0\kappa_{11})]/[c_{44}(\kappa_{11}\mu_{11}- \\
& d_{11}^2)+e_{15}^2(\mu_{11}-d_{11})+q_{15}e_{15}(\kappa_{11}-d_{11})]
\end{aligned}
$$

$$
\begin{aligned}
C_5 = {} & \{q_{15}\left(1+\frac{1}{\alpha_1}\right)[\tau_0(\kappa_{11}\mu_{11}-d_{11}^2)-e_{15}(D_0\mu_{11}- \\
& B_0 d_{11})+q_{15}(D_0 d_{11}-B_0\kappa_{11})]- \\
& 2d_{11}[c_{44}(D_0\mu_{11}-B_0 d_{11})+\tau_0 e_{15}(\mu_{11}-d_{11})+ \\
& q_{15}e_{15}(D_0-B_0)]-2\mu_{11}[c_{44}(\kappa_{11}B_0-d_{11}D_0)+ \\
& e_{15}^2(B_0-D_0)+\tau_0 e_{15}(\kappa_{11}- \\
& d_{11})]\}\ /\ [c_{44}(\kappa_{11}\mu_{11}-d_{11}^2)+ \\
& e_{15}^2(\mu_{11}-d_{11})+q_{15}e_{15}(k_{11}-d_{11})]
\end{aligned}
$$

$$
\begin{aligned}
C_6 = {} & q_{15}\left(1-\frac{1}{\alpha_1}\right)[\tau_0(\kappa_{11}\mu_{11}-d_{11}^2)-e_{15}(D_0\mu_{11}- \\
& B_0 d_{11})+q_{15}(D_0 d_{11}-B_0\kappa_{11})]/[c_{44}(\kappa_{11}\mu_{11}- \\
& d_{11}^2)+e_{15}^2(\mu_{11}-d_{11})+q_{15}e_{15}(\kappa_{11}-d_{11})]
\end{aligned}
$$

且

$$
\begin{aligned}
F(\zeta) = {} & \frac{1}{2\pi\mathrm{i}}\int_{|\sigma|=1}\frac{\omega'(\sigma)}{\sigma-\zeta}\mathrm{d}\sigma = \\
& \frac{2H}{\pi^2}\left[\frac{\sqrt{\alpha}}{\alpha(1-\zeta)^2+(1+\zeta)^2}\ln\frac{1+\sqrt{\alpha}}{1-\sqrt{\alpha}}-\right. \\
& \left.\frac{\sqrt{\alpha\gamma}}{\alpha\gamma(1-\zeta)^2+(1+\zeta)^2}\ln\frac{1+\sqrt{\alpha\gamma}}{1-\sqrt{\alpha\gamma}}\right]\frac{2H}{\pi^2}\cdot \\
& \frac{\mathrm{i}\alpha(1-\gamma)(1-\zeta^2)}{[\alpha\gamma(1-\zeta)^2+(1+\zeta)^2][\alpha\gamma(1-\zeta)^2+(1+\zeta)^2]}\cdot \\
& \ln\frac{\mathrm{i}-\zeta}{1-\mathrm{i}\zeta}
\end{aligned} \tag{16}
$$

## 2.2 应力强度因子求解

场强度因子可定义为

$$
\boldsymbol{K}_{\mathrm{III}} = \begin{bmatrix} K_\sigma \\ K_D \\ K_B \end{bmatrix} = \lim_{\zeta\to\zeta_0}\sqrt{2\pi[\omega(\zeta)-\omega(\zeta_0)]}\cdot \frac{F(\zeta)}{\omega'(\zeta)}\begin{bmatrix} \sigma_{32} \\ D_2 \\ B_2 \end{bmatrix} \tag{17}
$$

由式(15)和式(16)可得到运动状态下，两裂纹尖端(0,0)、($L$,0)处应力强度因子分别为

$$
\boldsymbol{K}_{\mathrm{III}}^{(0,0)} = \begin{bmatrix} \dfrac{1}{\alpha_1}\tau_0+\left(1-\dfrac{1}{\alpha_1}\right)\tau_1 \\ \dfrac{1}{\alpha_1}D_0+\left(1-\dfrac{1}{\alpha_1}\right)\dfrac{\kappa_{11}}{e_{15}}\tau_1 \\ \dfrac{1}{\alpha_1}B_0-\left(1-\dfrac{1}{\alpha_1}\right)\dfrac{d_{11}}{q_{15}}\tau_1 \end{bmatrix}\frac{\sqrt{2H}}{\pi\sqrt{1-\gamma}}\cdot \left[\ln\frac{1+\sqrt{\alpha}}{1-\sqrt{\alpha}}-\sqrt{\gamma}\ln\frac{1+\sqrt{\alpha\gamma}}{1-\sqrt{\alpha\gamma}}\right] \tag{18}
$$

$$
\boldsymbol{K}_{\mathrm{III}}^{(L,0)} = \begin{bmatrix} \dfrac{1}{\alpha_1}\tau_0+\left(1-\dfrac{1}{\alpha_1}\right)\tau_1 \\ \dfrac{1}{\alpha_1}D_0+\left(1-\dfrac{1}{\alpha_1}\right)\dfrac{\kappa_{11}}{e_{15}}\tau_1 \\ \dfrac{1}{\alpha_1}B_0-\left(1-\dfrac{1}{\alpha_1}\right)\dfrac{d_{11}}{q_{15}}\tau_1 \end{bmatrix}\frac{\sqrt{2H}}{\pi\sqrt{1-\gamma}}\cdot \left[\sqrt{\gamma}\ln\frac{1+\sqrt{\alpha}}{1-\sqrt{\alpha}}-\ln\frac{1+\sqrt{\alpha\gamma}}{1-\sqrt{\alpha\gamma}}\right] \tag{19}
$$

其中：

$$
\begin{aligned}
\tau_1 = {} & [q_{15}e_{15}(\kappa_{11}-d_{11})\tau_0+e_{15}^2(\mu_{11}-d_{11})\tau_0- \\
& c_{44}e_{15}(D_0\mu_{11}-B_0 d_{11})+c_{44}q_{15}(B_0\kappa_{11}- \\
& D_0 d_{11})]/[c_{44}(\kappa_{11}\mu_{11}-d_{11}^2)+e_{15}^2(\mu_{11}-d_{11})+ \\
& q_{15}e_{15}(\kappa_{11}-d_{11})]
\end{aligned}
$$

当左边裂纹的运动速度趋于零时，$\alpha_1\to 1$，所得结果退化为静态裂纹解：

$$
\boldsymbol{K}_{\mathrm{III}}^{(0,0)} = \alpha\begin{bmatrix} \tau_0 \\ D_0 \\ B_0 \end{bmatrix}\frac{\sqrt{2H}}{\pi\sqrt{1-\gamma}}\left(\ln\frac{1+\sqrt{\alpha}}{1-\sqrt{\alpha}}-\sqrt{\gamma}\ln\frac{1+\sqrt{\alpha\gamma}}{1-\sqrt{\alpha\gamma}}\right) \tag{20}
$$

$$
\boldsymbol{K}_{\mathrm{III}}^{(l,0)} = \begin{bmatrix} \tau_0 \\ D_0 \\ B_0 \end{bmatrix}\frac{\sqrt{2H}}{\pi\sqrt{1-\gamma}}\left(\sqrt{\gamma}\ln\frac{1+\sqrt{\alpha}}{1-\sqrt{\alpha}}-\ln\frac{1+\sqrt{\alpha\gamma}}{1-\sqrt{\alpha\gamma}}\right) \tag{21}
$$

当两裂纹尖端的距离 $L$ 为无穷大时式(19)化为

$$\boldsymbol{K}_{\mathrm{III}}^{(0,0)}=\begin{bmatrix}\dfrac{1}{\alpha_1}\tau_0+\left(1-\dfrac{1}{\alpha_1}\right)\tau_1\\ \dfrac{1}{\alpha_1}D_0+\left(1-\dfrac{1}{\alpha_1}\right)\dfrac{\kappa_{11}}{e_{15}}\tau_1\\ \dfrac{1}{\alpha_1}B_0-\left(1-\dfrac{1}{\alpha_1}\right)\dfrac{d_{11}}{q_{15}}\tau_1\end{bmatrix}\cdot \frac{\sqrt{2H}}{2\pi}\ln\frac{2\mathrm{e}^{\frac{\pi a}{H}}-1+2\mathrm{e}^{\frac{\pi a}{H}}\sqrt{1-\mathrm{e}^{\frac{-\pi a}{H}}}}{2\mathrm{e}^{\frac{\pi a}{H}}-1-2\mathrm{e}^{\frac{\pi a}{H}}\sqrt{1-\mathrm{e}^{\frac{-\pi a}{H}}}}\tag{22}$$

当 $\alpha_1\rightarrow 1$ 时，式(22)化为

$$\boldsymbol{K}_{\mathrm{III}}^{(0,0)}=\begin{bmatrix}\tau_0\\ D_0\\ B_0\end{bmatrix}\frac{\sqrt{2H}}{2\pi}\ln\frac{2\mathrm{e}^{\frac{\pi a}{H}}-1+2\mathrm{e}^{\frac{\pi a}{H}}\sqrt{1-\mathrm{e}^{\frac{-\pi a}{H}}}}{2\mathrm{e}^{\frac{\pi a}{H}}-1-2\mathrm{e}^{\frac{\pi a}{H}}\sqrt{1-\mathrm{e}^{\frac{-\pi a}{H}}}}\tag{23}$$

式(23)与文献[8]中的结果相一致。

### 2.3　能量释放率求解

定义能量释放率[16]为

$$G_{\mathrm{m}}^{(0,0)}=\frac{1}{2}[K_\sigma\ K_D\ K_B]R^{-1}\begin{bmatrix}K_\sigma\\ K_D\\ K_B\end{bmatrix}\tag{24}$$

其中：

$$R^{-1}=\begin{bmatrix}\kappa_{11}\mu_{11}-d_{11}^2 & e_{15}\mu_{11}-d_{11}q_{15} & \kappa_{11}q_{15}-d_{11}e_{15}\\ e_{15}\mu_{11}-d_{11}q_{15} & -q_{15}^2-c_{44}\mu_{11} & c_{44}d_{11}+e_{15}q_{15}\\ \kappa_{11}q_{15}-d_{11}e_{15} & c_{44}d_{11}+e_{15}q_{15} & -e_{15}^2-c_{44}\kappa_{11}\end{bmatrix}\cdot\frac{1}{\det\boldsymbol{D}}\tag{25}$$

$$\boldsymbol{D}=\begin{bmatrix}c_{44} & e_{15} & q_{15}\\ e_{15} & -\kappa_{11} & -d_{11}\\ q_{15} & -d_{11} & -\mu_{11}\end{bmatrix}\tag{26}$$

由式(17)、式(18)及式(23)可得到动态裂纹尖端处的机械应变能释放率为

$$G_{\mathrm{m}}^{(0,0)}=\left[\frac{1}{\alpha_1}\tau_0+(1-\frac{1}{\alpha_1})\tau_1\quad \frac{1}{\alpha_1}D_0+(1-\frac{1}{\alpha_1})\frac{\kappa_{11}}{e_{15}}\tau_1\quad \frac{1}{\alpha_1}B_0-(1-\frac{1}{\alpha_1})\frac{d_{11}}{q_{15}}\tau_1\right]\cdot R^{-1}\begin{bmatrix}\dfrac{1}{\alpha_1}\tau_0+(1-\dfrac{1}{\alpha_1})\tau_1\\ \dfrac{1}{\alpha_1}D_0+(1-\dfrac{1}{\alpha_1})\dfrac{\kappa_{11}}{e_{15}}\tau_1\\ \dfrac{1}{\alpha_1}B_0-(1-\dfrac{1}{\alpha_1})\dfrac{d_{11}}{q_{15}}\tau_1\end{bmatrix}\cdot\frac{H}{\pi^2(1-\gamma)}\cdot\left(\ln\frac{1+\sqrt{\alpha}}{1-\sqrt{\alpha}}-\sqrt{\gamma}\ln\frac{1+\sqrt{\alpha\gamma}}{1-\sqrt{\alpha\gamma}}\right)^2\tag{27}$$

$$G_{\mathrm{m}}^{(L,0)}=\left[\frac{1}{\alpha_1}\tau_0+(1-\frac{1}{\alpha_1})\tau_1\quad \frac{1}{\alpha_1}D_0+(1-\frac{1}{\alpha_1})\frac{\kappa_{11}}{e_{15}}\tau_1\quad \frac{1}{\alpha_1}B_0-(1-\frac{1}{\alpha_1})\frac{d_{11}}{q_{15}}\tau_1\right]\cdot R^{-1}\begin{bmatrix}\dfrac{1}{\alpha_1}\tau_0+(1-\dfrac{1}{\alpha_1})\tau_1\\ \dfrac{1}{\alpha_1}D_0+(1-\dfrac{1}{\alpha_1})\dfrac{k_{11}}{e_{15}}\tau_1\\ \dfrac{1}{\alpha_1}B_0-(1-\dfrac{1}{\alpha_1})\dfrac{d_{11}}{q_{15}}\tau_1\end{bmatrix}\tag{28}$$

当裂纹传播速度趋于零时，$\alpha_1\rightarrow 1$，式(26)和式(27)退化为静态下的能量释放率：

$$\begin{cases}G_{\mathrm{m}}^{(0,0)}=\dfrac{\Lambda}{\det\boldsymbol{D}}\dfrac{H}{\pi^2(1-\gamma)}\left[\ln\dfrac{1+\sqrt{\alpha}}{1-\sqrt{\alpha}}-\sqrt{\gamma}\ln\dfrac{1+\sqrt{\alpha\gamma}}{1-\sqrt{\alpha\gamma}}\right]^2\\ G_{\mathrm{m}}^{(L,0)}=\dfrac{\Lambda}{\det\boldsymbol{D}}\cdot\dfrac{H}{\pi^2(1-\gamma)}\left(\sqrt{\gamma}\ln\dfrac{1+\sqrt{\alpha}}{1-\sqrt{\alpha}}-\ln\dfrac{1+\sqrt{\alpha\gamma}}{1-\sqrt{\alpha\gamma}}\right)^2\end{cases}\tag{29}$$

其中：

$$\Lambda=\tau_0^2(\kappa_{11}\mu_{11}-d_{11}^2)-D_0^2(q_{15}^2+c_{44}\mu_{11})-B_0^2(e_{15}^2+c_{44}\kappa_{11})+2\tau_0D_0(e_{15}\mu_{11}-d_{11}q_{15})+2\tau_0B_0(\kappa_{11}q_{15}-d_{11}e_{15})+2D_0B_0(c_{44}d_{11}+e_{15}q_{15})\tag{30}$$

当两裂纹尖端的距离 $L\rightarrow\infty$ 时 $\gamma\rightarrow 0$，式(28)化为

$$G_{\mathrm{m}}^{(0,0)}=\frac{\Lambda}{\det\boldsymbol{D}}\frac{H}{4\pi^2}\left(\ln\frac{2\mathrm{e}^{\frac{\pi a}{H}}-1+2\mathrm{e}^{\frac{\pi a}{H}}\sqrt{1-\mathrm{e}^{\frac{-\pi a}{H}}}}{2\mathrm{e}^{\frac{\pi a}{H}}-1-2\mathrm{e}^{\frac{\pi a}{H}}\sqrt{1-\mathrm{e}^{\frac{-\pi a}{H}}}}\right)^2\tag{31}$$

式(31)的结果也与文献[8]的对应结果相一致。

### 2.4　实例计算

选取磁电弹性复合材料 $BaTiO_3$-$CoFe_2O_4$，其中压电相为 $BaTiO_3$，压磁相为 $CoFe_2O_4$。同文献[8]一样，采用了文献[17]中提供的 $BaTiO_3$-$CoFe_2O_4$ 的参数，如表 1 所示。

设临界能量释放率为 $G_{\mathrm{cr}}=5.0\ \mathrm{N/m}$，受载裂纹的长度为 $a=0.01\ \mathrm{m}$。图 2 为狭长磁电弹性体中宽度与受载裂纹长度之比 $H/a$ 对两裂纹能量释放率 $G_{\mathrm{m}}^{(0,0)}/G_{\mathrm{cr}}$ 和 $G_{\mathrm{m}}^{(\mathrm{L},0)}/G_{\mathrm{cr}}$ 的影响。可以看出，左边受载荷裂纹的能量释放率随着狭长体宽度 $H$ 的增加而减小，且趋于常数，右边裂纹的能量释放率随 $H$ 的增加只有微弱增加。当该材料体的宽度与受载荷裂纹长度比 $H/a\leqslant 2.5$ 时，狭长体宽度的变化对左裂纹能量释放率的影响很大，而当 $H/a>2.5$ 时，狭长体宽度 $H$ 对左裂纹能量释放率的影响

**表 1　$BaTiO_3$-$CoFe_2O_4$ 的参数**

**Table 1　Parameters of $BaTiO_3$-$CoFe_2O_4$**

| Piezoelectric constant $e^{15}/(\mathrm{C\cdot m^{-2}})$ | Elastic constant $c_{44}$ /Pa | Dielectric permittivity $\kappa_{11}/(\mathrm{C^2\cdot N^{-1}\cdot m^{-2}})$ | Piezomagnetic constant $q_{15}/(\mathrm{N^{-1}\cdot A^{-1}\cdot m^{-1}})$ | Magnetic permeability $\mu_{11}/(\mathrm{N\cdot s^2\cdot C^{-2}})$ | Magnetoelectric coupling constant $d_{11}/(\mathrm{N\cdot s\cdot V^{-1}\cdot C^{-1}})$ |
|---|---|---|---|---|---|
| 5.8 | $4.4\times10^{10}$ | $5.64\times10^{-9}$ | $2.75\times10^{2}$ | $2.97\times10^{-4}$ | $5.2\times10^{-12}$ |

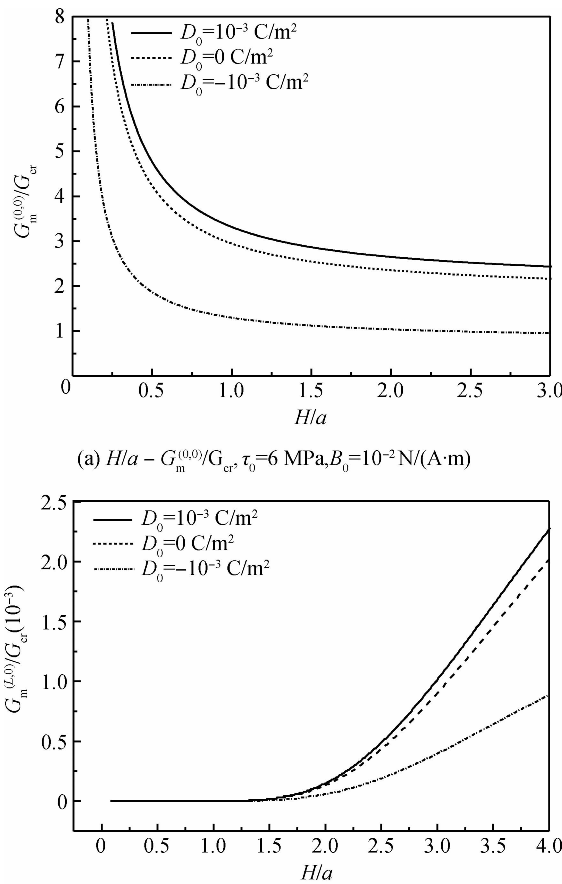


(a) $H/a-G_m^{(0,0)}/G_{cr}$, $\tau_0$=6 MPa, $B_0=10^{-2}$ N/(A·m)

(b) $H/a-G_m^{(L,0)}/G_{cr}$, $\tau_0$=6 MPa, $B_0=10^{-2}$ N/(A·m)

图 2　狭长磁电弹性体中 $H/a$ 对 $G_m^{(0,0)}/G_{cr}$ 和 $G_m^{(L,0)}/G_{cr}$ 的影响

Fig. 2　Effects of $H/a$ in magnetoelectroelastic strip on $G_m^{(0,0)}/G_{cr}$ and $G_m^{(L,0)}/G_{cr}$

很小。若 $H$ 固定，随受载裂纹长度 $a$ 增大，左裂纹的能量释放率增大，右边裂纹的能量释放率微弱减小。

取 $a=0.01$ m，$H=0.05$ m，图 3 为外载荷、电场、磁场分别对 $G_m^{(0,0)}/G_{cr}$ 的影响。可以看出，外力的作用可促进裂纹扩展，电场的作用可使能量释放率增大，磁场相对于能量释放率的变化率几乎为零。图 4 为两裂纹的间距与狭长体宽度之比 $L/H$ 对两裂纹能量释放率 $G_m^{(0,0)}/G_{cr}$ 和 $G_m^{(L,0)}/G_{cr}$ 的影响。可以看出，当 $H$ 固定时，左右两边裂纹的能量释放率均随着两裂纹之间的距离 $L$ 的增加而减小，最后趋于一定值。

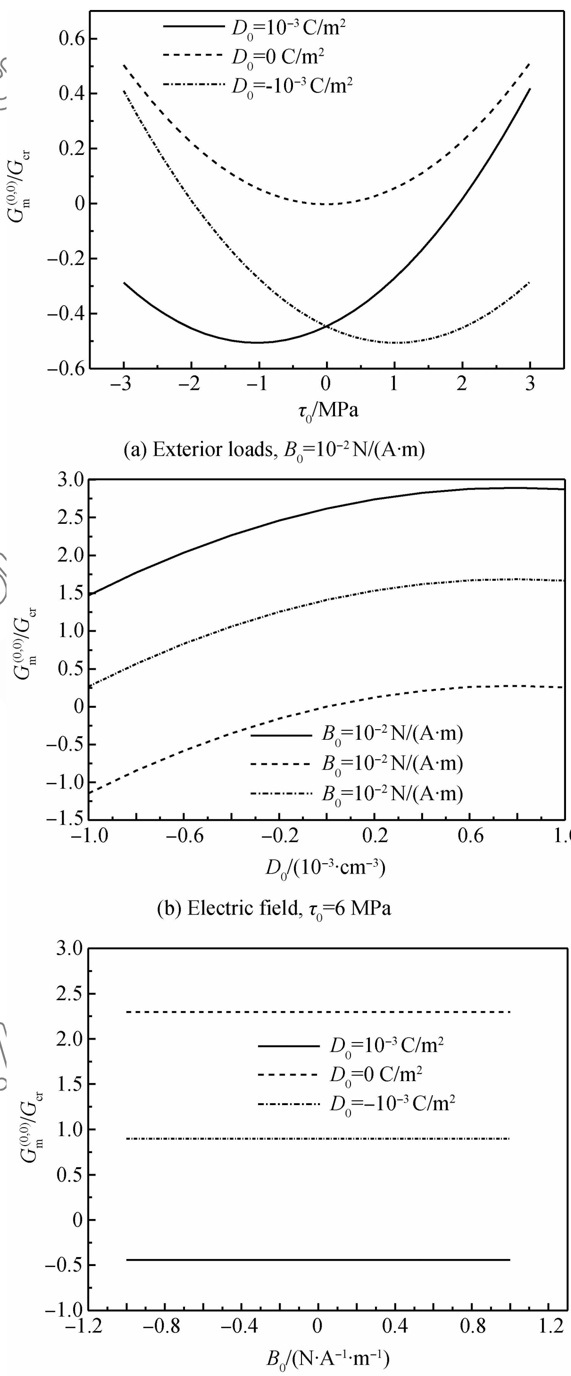


(a) Exterior loads, $B_0=10^{-2}$ N/(A·m)

(b) Electric field, $\tau_0$=6 MPa

(c) Magnetic field, $\tau_0$=6 MPa

图 3　外载荷、电场、磁场分别对 $G_m^{(0,0)}/G_{cr}$ 的影响

Fig. 3　Effects of exterior loads, electric field and magnetic field on $G_m^{(0,0)}/G_{cr}$

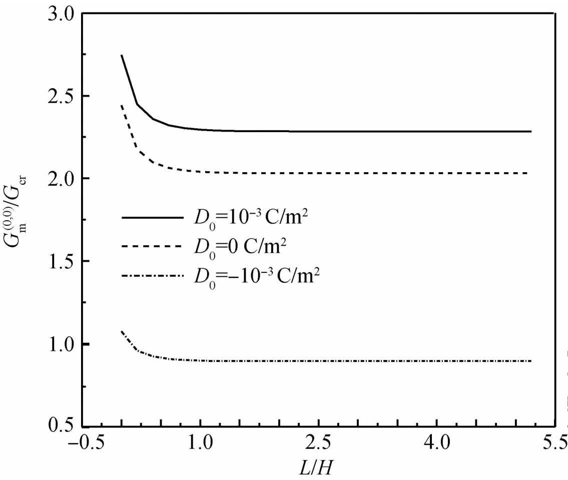


(a) $L/H-G_m^{(0,0)}G_{cr}$, $\tau_0$=6 MPa, $B_0=10^{-2}$ N/(A·m)

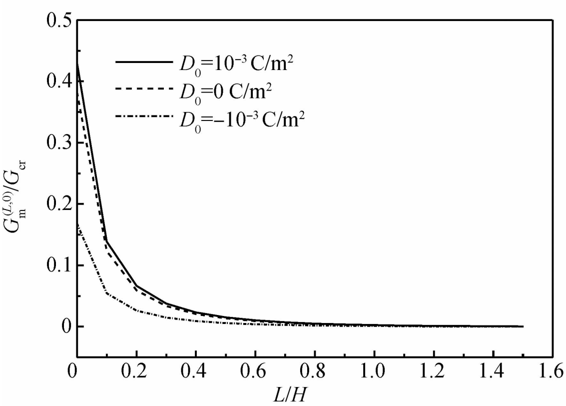


(b) $L/H-G_m^{(L,0)}G_{cr}$, $\tau_0$=6 MPa, $B_0=10^{-2}$ N/(A·m)

图 4　$L/H$ 对 $G_m^{(0,0)}/G_{cr}$ 和 $G_m^{(L,0)}/G_{cr}$ 的影响

Fig. 4　Effects of $L/H$ on $G_m^{(0,0)}/G_{cr}$ and $G_m^{(L,0)}/G_{cr}$

## 3　结　论

对于边界条件是磁非渗透和电非渗透型的有限宽条形磁电弹性体，含有两条无限长共线裂纹问题，推出了裂纹尖端的动态应力强度因子及能量释放率的精确解。当裂纹传播速度趋于零时，退化为有限宽条形磁电弹性体中静态的双半裂纹问题。当 $L\to\infty$ 时，狭长体中的双裂纹问题便退化为单裂纹问题，式(18)与式(24)所得结果与文献[8]中的结果相一致。通过实例计算，得出了在静止状态下狭长体及裂纹的若干几何尺寸及电、力及磁等载荷分别对能量释放率的影响规律，得出如下结论。

(1) 磁电弹性狭长体的几何尺寸 $H/a\leqslant 2.5$ 时，左裂纹的能量释放率随狭长体宽度的变大而减小，右裂纹能量释放率几乎没有影响。$H/a>2.5$ 时，狭长体宽度的变大对左裂纹能量释放率的影响较小，右裂纹能量释放率只是微弱增加。若 $H$ 无限增大时，受载裂纹的能量释放率趋于常数。表明条形磁电弹性复合材料体加宽可阻止裂纹的扩展。在狭长体宽度固定时，随受载裂纹长度的增加，左裂纹的能量释放率明显加大，容易造成基体的断裂。当 $H$ 固定时，左右两边裂纹的能量释放率均随着两裂纹之间距离 $L$ 的增加而减小，最终趋于一定值，双裂纹问题随即退化成单裂纹问题。右边无载荷裂纹的存在对基体的稳定性影响不大。

(2) 纯机械载荷始终促进裂纹扩展，负电场使能量释放率变小，正电场使能量释放率增加到一定数值后再变小，说明负电场对裂纹扩展有阻止作用，正电场达到一定值后对裂纹扩展也有阻止作用。磁场对能量释放率的影响不明显，这与单裂纹的情况基本类似。

## 参考文献：


[1]　Van Suchtelen J. Product properties: A new application of composite materials[J]. Philips Research Reports, 1972, 27(1): 28-37.

[2]　Hou P F, Leung A Y T. A spheroidal inclusion in an infinite magneto-electro-elastic material [J]. International Journal of Engineering Science, 2004, 42(11-12): 1255-1273.

[3]　Wang X, Shen Y P. Inclusions of arbitrary shape in magneto-electroelastic composite materials[J]. International Journal of Engineering Science, 2003, 41(1): 85-102.

[4]　Liu J X, Liu X L, Zhao Y B. Green's function for anisotropic magnetoelectroelastic solids with an elliptical cavity or a crack[J]. International Journal of Engineering Science, 2001, 39: 1405-1418.

[5]　Wang B L, Mai Y W. Fracture of piezoelec-tromagnetic materials[J]. Mechanics Research Communication, 2004, 31(1): 65-73.

[6]　Zhang Z K, Soh A K. Micromechanics preditions of the effective moduli of magnctoelectroelastic composite materials [J]. European Journal of Mechanics - A/Solids, 2005, 24: 1054-1067.

[7]　Soh A K, Liu J X. Mode III interfacial edge crack in a magnetoelectroelectroelastic biomaterial [J]. Key Engineering Materials, 2004, 261-263: 393-398.

[8]　Guo J H, Lu Z X, Siri G L. Field intensity factors of a model-III semi-infinite crack in amagnetoelectroelastic strip[J]. Acta Materiae Compositae Sinica, 2013, 30(4): 136-143(in Chinese).
郭俊宏，卢子兴，斯日古楞. 狭长磁电弹性体中 III 型半无限裂纹的场强度因子[J]. 复合材料学报, 2013, 30(4): 136-143.

[9]　Hu K Q, Zhong Z. A moving mode-III crack in a functionally graded piezoelectric strip[J]. International Journal of Me-

chanics and Materials in Design，2005，2(1-2)：61-79.

[10] Yan Z，Jiang L Y. Study of a propagating finite crack in functionally graded piezoelectric materials considering dielectric medium effect[J]. International Journal of Solids and Structures，2009，46(6)：1362-1372.

[11] Singh B M，Rokne J，Dhahwal R S. Closed form solutions for two anti-plane collinear cracks in a magnetoelectroelastic layer [J]. European Journal of Mechanics A，2009，28(3)：599-609.

[12] Hu K Q，Li G Q，Zhu B B. Electro-magneto-elastic analysis of a piezoelectromagnetic strip with a finite crack under longitudinal shear [J]. Engineering Mechanics，2006，23(5)：168-172 (in Chinese).
胡克强，李国强，朱保兵. 压电-压磁板条中反平面裂纹的电-磁-弹性分析[J]. 工程力学，2006，23(5)：168-172.

[13] Lu Z X，Liu P，Guo J H. Exact soluteons of two semiinfinite collinear cracks in piezo electric strip[J]. Applied Mathematics and Mechanics，2011，32(11)：1399-1406.

[14] Liu P，Yuan Z S，Lu Z X. Finite strip analysis of semi infinite piezoelectric body moving crack problem solution[C]//the Twenty-second National Conference on Structural Engineering III Album. Beijing："Engineering Mechanics" Magazine. 2013：505-508 (in Chinese).
刘萍，袁泽帅，卢子兴. 有限高狭长压电体中半无限运动裂纹问题解析解[C]//第22届全国结构工程学术会议论文集，北京：工程力学杂志社，2013：505-508.

[15] Shen D W，Fan T Y. Exact solutions of two semi-infinite collinear cracks in a strip [J]. Engineering Fracture Mechanics，2003，70(2)：813-822.

[16] Zhong X C. Study on fracture of magnetoelectroelastic[D]. Changsha：Zhong Nan University，2008(in Chinese).
钟献词. 磁电弹性介质的断裂问题研究[D]. 长沙：中南大学，2008.

[17] Li X F. Dynamic analysis of a cracked magnetoelectroelastic medium under anti-plane mechanical and in-plane electric and magnetic impacts [J]. International Journal of Solids and Structures，2005，42(11-12)：3185-3205.

## Dynamic and static analysis for two semi-infinite cracks in finite magnetoelectroelastic strip

GUO Huaimin*，ZHAO Guozhong

(Mathematic Science College，Baotou Teachers College，Baotou 014030，China)

**Abstract**： The crack in strip is often used in fracture mechanics as research model. There is a magnetoelectroelastic elastomer which contains infinite collinear cracks，when crack surface on the left side near crack tip is under the electromagnetic force load and anti-plane shear stress along the crack surface，elastomer tends to produce dynamic fracture. By using arch transform formula of complex variable function method，the analytic solutions of the dynamic stress intensity factors and the mechanical strain energy release rate were presented with the boundary conditions that the surface of the crack was electrically and magnetically impermeable. When the movement velocity tends to zero，the analytic solutions is degraded to stationary state solution. Through numerical example，the fracture mechanism was analyzed，the influence of the geometry size of strip and crack，external force，electric field and magnetic field on energy release rate respectively under static state were discussed to help the design and manufacture of related devices.

**Keywords**： movement cracks；magnetoelectroelastic composites；complex function method；stress intensity factors；mechanical strain energy release rate